The Dynamic Coupling Between the Pulse Wake Mixing Strategy and Floating Wind Turbines

Daniel van den Berg[1], Delphine de Tavernier[2], and Jan-Willem van Wingerden[1]

[1]Delft Center for Systems and Control, Delft University of Technology, Mekelweg 2, 2628 CD Delft, The Netherlands
[2]Department of Flow Physics and Technology, Delft University of Technology, Kluyverweg 1, 2629 HS Delft, The Netherlands

Correspondence: Daniel van den Berg (d.g.vandenberg@tudelft.nl)

Abstract. In recent years control techniques such as dynamic induction control (often referred to as "The Pulse") have shown great potential in increasing wake mixing with the goal of minimizing turbine-to-turbine interaction within a wind farm. Dynamic induction control disturbs the wake by varying the thrust of the turbine over time, which results in a time-varying induction zone. If applied to a floating wind turbine, this time-varying thrust force will, besides changing the wake, change the

5 motion of the platform. This work investigates if the coupling between the Pulse and floater dynamics has an impact on the wake mixing performance of the Pulse. This is done by considering first the magnitude of motions of the floating wind turbine due to the application of a time-varying thrust force and secondly the effect of these motions on the wake mixing. A frequency response experiment shows that the movement of the floating turbine is heavily frequency-dependent, as is the thrust force. Time domain simulations, using a free wake vortex method with uniform inflow, show that the expected gain in average wind

10 speed at a distance of five rotor diameters downstream is more sensitive to the excitation frequency compared to a bottom-fixed turbine with the same Pulse applied. This is due to the fact that platform motion decreases the thrust force variation and thus reduces the onset of wake mixing.

1 Introduction

The drive for the European Union (EU) to become carbon-neutral and energy self-sufficient has increased the demand for re-

15 newable energy production. These goals were (re)formulated in the REPowerEU Plan (European Commission, 2022). Offshore wind energy is often regarded as one of the key technologies to provide this green renewable energy (Panwara et al., 2011). As of 2021, offshore wind farms provided 28 GW (13.5%) of the 236 GW of installed wind capacity in Europe. These offshore wind farms are all located in shallow (less than 50 m) waters (Komusanac et al., 2021; Ramirez et al., 2020). However, to achieve the 480 GW of installed wind capacity (on- and offshore combined) target by 2030 (European Commission, 2022),

20 offshore wind needs to find access to the deeper waters of the European Union, and the United Kingdom, where 80% of the total wind energy resources can be found (WindEurope, 2017). Floating wind turbines (FWTs) will play a key role in enabling access to these energy resources. As the technology matures, floating turbines will likely be clustered into large wind farms, similar to the bottom-fixed wind farms in shallower waters.

It is well-known that wind turbines within a wind farm interact with the wakes of surrounding turbines. This results in an extensive reduction of the power production of the individual turbines, which may be in the order of 10 to 25% (Barthelmie et al., 2009, 2010). Since wake interaction is a major source of energy loss, a significant amount of research has been performed on understanding wake effects. In steady design and operational conditions, considerable advances have been made since the first engineering method presented by Jensen (1983). However, particularly in unsteady inflow or operational conditions that are inevitable for floating turbines, wake losses and mitigation techniques remain elusive.

With this work, we will study to what extent the wake losses of floating wind turbines can be minimized using dynamic induction control techniques. In particular, we will look at the Pulse wake mixing technique. More specifically, we will consider if floating wind turbines can leverage their extra degrees of freedom while using this wake mixing strategy.

1.1 Background

For bottom-fixed turbines, various strategies have been proposed in the literature in order to reduce wake losses. These strategies include wind farm layout optimization, steady-state control solutions and active wake control strategies (Meyers et al., 2022).

Since the introduction of (engineering) wake models, the placement of wind turbines within a wind farm has received major attention, typically for the goal of wind farm layout optimization. The work by Mosetti et al. (1994) and Petersen et al. (1998) show that optimizing the layout of the wind farm for a given type of turbine, plot size and historic wind information is possible. More recently, Kirchner-Bossi and Porté-Agel (2018) achieved an increase in power production in the order of 2% simulating two real-world wind farms for which the turbines have been redistributed using genetic optimization algorithms. These approaches assume the turbine to be static, where the only degree of freedom is the placement of the turbine with respect to each other. As input to the optimization, historical wind data is used to maximize the potential power gain for the prevailing wind. Because the optimization is static, this potential gain is limited for wind directions that occur less often.

A different approach considers using an optimal steady-state control solution using the available degrees of freedom of a bottom-fixed turbine. The two methods that have gained traction in literature are wake re-direction and induction control. Using the yawing availability of the turbine, the rotor can be statically misaligned with the mean wind direction to divert the wake away from downstream turbines. This increases the power output of downwind turbines at the cost of power loss on the upwind turbine for an overall net gain (Jiménez et al., 2010; Bastankhah and Porté-Agel, 2016; Gebraad et al., 2016). A downside of this method is that, as the number of wind turbines in a farm increases, a diverted wake for one pair of turbines could overlap with a different turbine. Furthermore, the yawed turbine will experience increased loading which reduces the turbine's lifetime (Fleming et al., 2015). Yaw misalignment is an example of *steady-state* optimal control. The use of a model, such as FLORIDyn (Becker et al., 2022; Gebraad and van Wingerden, 2014), allows calculating an optimal yaw angle based on measurements within a wind farm. Once the turbine is positioned in the new desired configuration, it is kept steady until the wind conditions change.

Steady-state induction control (also called de-rating control) is another approach used to increase farm output. It uses the induction factor of the turbine as a control input. Similar to wake re-direction, the performance of the first turbine is sacrificed for the benefit of downwind turbines. Induction control has shown great potential in different simulation and optimization

environments (Marden et al., 2013; Ciri et al., 2017). However, wind tunnel experiments and full-scale experiments have shown that the gain of induction control is negligible (Campagnolo et al., 2016; van der Hoek et al., 2019), contrary to what is found using wake re-directing (Campagnolo et al., 2016). Similar results were found in a full-scale experiment (Fleming et al., 2017).

As an alternative to the steady-state optimal control techniques, new forms of active, time-varying, control have gained interest within the scientific community and were first introduced by Goit and Meyers (2015). As a result of this research, two notable active control techniques have emerged: the Pulse (formally Dynamic Induction Control or DIC) (Munters and Meyers, 2016, 2018) and the Helix (formally Dynamic Individual Pitch Control or DIPC) (Frederik et al., 2020a). Both methods rely on disturbing the wake using dynamic blade pitching such that the natural mixing process starts at an earlier distance downstream. For the Pulse wake mixing approach, the blade pitch angle of all rotor blades is varied collectively in a sinusoidal manner. For the Helix strategy, on the other hand, the blade pitch angle of the blades is controlled individually and varies sinusoidally with a phase offset between the blades. Both methods have shown in simulations to increase the power of a two-turbine wind farm by up to 5% for the Pulse and up to 7.5% for the Helix under turbulent inflow conditions (Frederik et al., 2020a).

The proposed techniques to mitigate wake interaction between turbines can also be applied to floating wind turbines. In fact, where bottom-fixed turbines are limited to one degree of freedom (yawing), a floating turbine has the ability to move in all six degrees of freedom. In general, these motions add significant complexity to the design of floating wind turbines, but for wake control purposes, they can potentially be leveraged. Moving turbines could be used for the purpose of repositioning the wind farm, and thus for active layout optimisation. This idea is used by Kheirabadi and Nagamune (2020) and Rodrigues et al. (2015) to actively optimize a wind farm based on wind conditions. In Kheirabadi and Nagamune (2020) several wind farms of differing sizes, placed in a grid layout with a 7-rotor diameter ('7D') spacing between turbines, are optimized. In their research, they showed that the overall farm efficiency could be increased by 5-10% by actively optimizing the layout, where the actual percentage of gain depends heavily on wind farm size and wind direction. Further, for certain types of floater designs, the orientation of the turbine can be changed by changing the ballast. This is done by Nanos et al. (2020), where wake deflection is realized by pitching the platform instead of yawing the turbine. Here, the wake deflects either upwards or downwards, where re-directing the wake downwards showed to increase the overall power production of a two-turbine wind farm (Nanos et al., 2020).

When wake mixing techniques such as the Pulse and Helix are used, the thrust force will vary over time. The research presented in Han and Nagamune (2020) and Kheirabadi and Nagamune (2020) showed that the thrust of the turbine can be used to alter the state of the floating turbine, and the platform to translate and/or rotate. For the Helix wake mixing technique, this is explored in van den Berg et al. (2022). In their work, the yaw moment originating from the Helix, is found to primarily excite the yaw degree of freedom of a floating turbine. By enabling the platform motion in yaw during Helix operation, the wind speed downstream increased by up to 10%, compared to a bottom-fixed turbine with the same Helix operation. Furthermore, it was found that the floating turbine, using the Helix, showed a similar performance as a bottom-fixed turbine, using the Helix with double the pitching amplitude. This gain is thought to originate from the fact that not only the wake is mixed but also

dynamically deflected. Further research is required to confirm this statement. For the Pulse wake mixing technique, it is not yet clear if a similar positive coupling between wake mixing technique and floater dynamics exists.

1.2 Research objective

95 The main contributions of this paper are twofold: (i) a frequency analysis of the motions of the floating turbine and its coupling to the Pulse dynamics, and (ii) time domain simulations to investigate the effect of the motions on wake mixing with the system represented by its full non-linear dynamics. These simulations are executed in *QBlade-Ocean* (Marten, 2022), a simulation suite capable of fully simulating hydro-, aero-elastics and wake dynamics. The wake is modelled using a free-wake vortex model.

The remainder of this paper is organized as follows: Section 2 introduces the simulation tool and settings used in this 100 research. Section 3 gives a short summary of the Pulse wake mixing technology. It also provides insight, using frequency response functions, into the dynamics of a floating turbine when exposed to the Pulse. Section 4 gives time domain results for the floating NREL 5MW turbine with the Pulse at three different frequencies. Finally, Section 5 will present the conclusion of this work.

2 Simulation tools and Research Methodology

105 In this research, *QBlade-Ocean* is used as the simulation tool (Marten, 2022). *QBlade-Ocean* uses a free-wake vortex method to simulate the flow field, and thus also the wake, around a turbine. The vortex method is known for its accuracy in the near wake (Leishman et al., 2002, 2004), as well as being computationally more efficient than comparable LES methods (Shaler et al., 2020). However, free-wake vortex methods are prone to numerical instability, especially in the far-wake region. Nevertheless, the vortex method can be used to analyze the wake further downstream, see for example (Marten et al., 2020; Rodriguez 110 et al., 2021). *QBlade-Ocean* is used as it is able to simulate both the hydrodynamics, as well as the near- to mid-wake.

Throughout this research, without loss of generality, the NREL 5MW turbine (Jonkman et al., 2009) mounted on an OC3 spar-buoy (Jonkman, 2010) is used. This floating wind turbine design has been extensively verified against OpenFast calculations and experimental data within the Floatech project (Floatech, 2022).

2.1 Numerical set-up

115 In this section, the settings used in *QBlade-Ocean* will be motivated. As for any aerodynamic simulation, the chosen settings are a trade-off between computational time and accuracy. In a free-wake vortex method, this trade-off is primarily dictated by the number of vortex elements in the wake, as computational time grows exponentially with the number of wake elements. The settings that influence computational time and accuracy can be divided into two groups. The first directly regulates the number of elements in the wake and is categorized under wake modelling in *QBlade-Ocean*. In the second group are settings that 120 influence vortex modelling. These settings generally have a larger impact on the accuracy of the wake and less on computational efficiency. Finally, the blade and time step discretization will also influence the number of vortex elements released into the
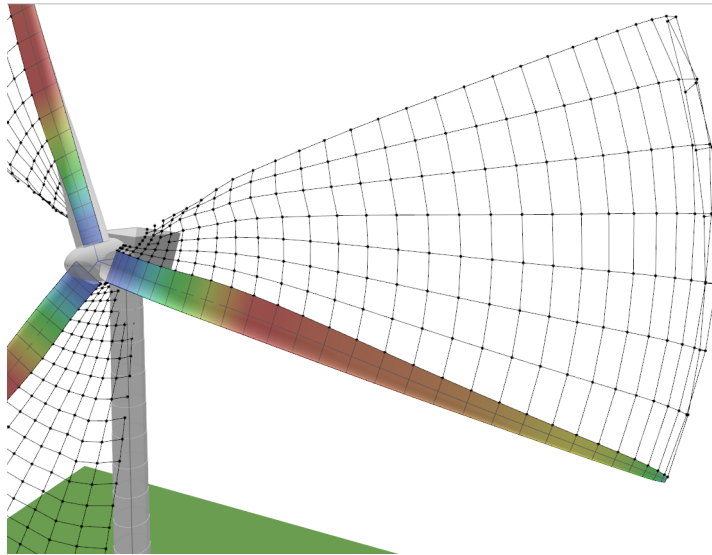
Figure 1. A close-up of the discretized blades and near-wake in QBlade-Ocean. The image is taken at the start of the simulation at which only the near wake is visible.

Table 1. Numerical simulation settings that regulate the wake discretization. These settings are used for all simulations presented in this paper.

Wake Modeling	Setting
Wake Relaxation	1 (No relaxation)
Max. Wake Elements	200000 [-]
Max. Wake Distance	100 Rotor Diameters
Wake Reduction Factor	0.001 [-]
Near Wake Length	0.5 Revolutions
Wake Zone 1/2/3 Length	6/12/6 Revolutions

wake and therefore will also have an impact on computational time and accuracy. Figure 1 shows an image of *QBlade-Ocean* with the fully panelised near wake visible.

125 The wake modelling settings are summarized in Table 1. These settings all directly influence the length of the wake and as such also the number of wake elements. The wake is cut-off when either the maximum number of wake elements or the maximum wake distance is reached. Wake relaxation, when enabled, blends the starting vortex and influences the length of the wake. When enabled, the resulting wake is too short for the analysis in this work, hence, for this reason, it is disabled. The wake reduction factor dictates when wake elements are removed based on their current vorticity strength compared to newly released vortices. The full wake is subdivided into four distinct areas. Of this, the near wake is a finely resolved wake close

130 to the turbine which mainly influences the performance of the turbine. Typically, the near wake does not need to be resolved

Table 2. Numerical simulation settings related to the aerodynamic modelling and vortex definition. These settings are used for all simulations presented in this work.

Vortex Modelling Settings	Setting
Initial Core Radius	0.05% Chord
Vortex Viscosity	1100 [-]
Vortex Strain	Disabled
Trailing Vortices	Enabled
Shed Vortices	Enabled

much further than half a rotor diameter for accurate results (Shaler et al., 2020). After the near wake, the wake transitions to wake zone 1. Wake zone 1, and consecutively wake zones 2 and 3, are regions in which the wake is increasingly sparsely resolved. When the wake transitions to a different zone, vortex filaments are merged to reduce the number of elements, which increases computational efficiency. The wake zones are defined in terms of revolutions of the turbine, which, based on the

135 average velocity in the wake, can be translated to a distance. Based on an in-depth grid study, the values in Table 1 were found to give a good trade-off between wake accuracy and computational time. Appendix A provides more detail on the effect of different wake zones on the velocity in the wake.

Settings that influence the vortex modelling are summarized in Table 2. The size of the core radius influences the stability of the wake, the larger the core radius the higher the stability. However, having a too-large core size can also limit the wake

140 mixing dynamics. Vortex viscosity is set to 1100, which was found to work well for modelling large rotors (Ananthan and Leishman, 2004; Berdowski, 2018). Finally, having both trailing and shed vortices increases the accuracy of the wake.

Table 3 summarizes key settings for the blade modelling. For each simulation, the time step is set to 0.05 [s]. With an inflow speed of 9 [m/s], the azimuthal step of the turbine is $\Delta\psi = 3.3°$ at rated speed. This azimuthal step was found to be a good compromise between accuracy and computation time (Shaler et al., 2020). Finally, the blade is discretized in 18 panels, which

145 are sinusoidally distributed over the blade. Appendix A shows, through a convergence study, that this yields accurate results and prevents a large increase in computational time. The simulation is run with the Beddoesh-Leishman unsteady aerodynamic model with the corresponding coefficients based on the research presented in Leishman et al. (1986). These values were validated using data from the MEXICO campaign in (Pereira et al., 2013).

3 The Pulse and Platform Dynamics

150 This section will summarize the driving principle behind the Pulse wake mixing mechanism. It also provides an analysis of the motions of a floating turbine initiated by the Pulse. This analysis is done based on frequency response functions (Astrom and Murray, 2008). The frequency responses provide insight into how the hydrodynamics of the floating turbine is coupled to the dynamics of the Pulse.

Table 3. Numerical simulation settings related to the turbine modelling. These settings are used for all simulations presented in this work.

Turbine Settings	Setting
Dynamic Stall Model	Beddoesh-Leishman
Pressure Lag Constant	1.7 [-]
Viscous Lag Constant	3.0 [-]
Time Step	0.05 [s]
Azimuthal Step	$\Delta \psi = 3.3°$ [deg]
Inflow Velocity	9 [m/s]
Discretization Panels #	18 [-]
Discretization Method	Sinusoidal

3.1 The Pulse Wake Mixing Strategy

155 The principle of the Pulse is derived from the work of Goit and Meyers (2015) and Munters and Meyers (2018) in which a global optimization for an entire wind farm provided an optimal thrust coefficient C_t' input for the wind turbines with the aim of power maximization. From the optimized wind field, temporal variations in shed vorticity were identified which disrupted the wake. This behaviour in the wake can be mimicked by adding a constant offset to the Betz-optimal coefficient, $C_t' = 2$, which can be expressed as Equation 1:

$$C_t'(t) = 2 + A \sin\left(2\pi St \frac{V_\infty}{D} t\right), \tag{1}$$

160

$$\text{with: } St = \frac{f_e D}{V_\infty}, \tag{2}$$

where A is the amplitude [-], D the rotor diameter in [m], V_∞ the inflow velocity in [m/s] and St is the Strouhal number [-], in which f_e is the pitching frequency in Hz. Finally, t is the time in [s]. With this time-varying thrust coefficient, the overall thrust force on the rotor will vary in a sinusoidal manner. In this paper we adopt the strategy proposed in (Frederik et al., 2020b). The

165 time-varying thrust force as described in Equation 1 can be realized by pitching the turbine blades with a similar sinusoidal signal.

3.2 Floater Dynamics

To capture the behaviour of the OC3 platform (Jonkman, 2010), several frequency response simulations are performed. The Pulse is applied at different frequencies after which the floating turbine reaches steady-state behaviour. Using the steady-state

170 signals, the gain and phase between input and outputs can be mapped.
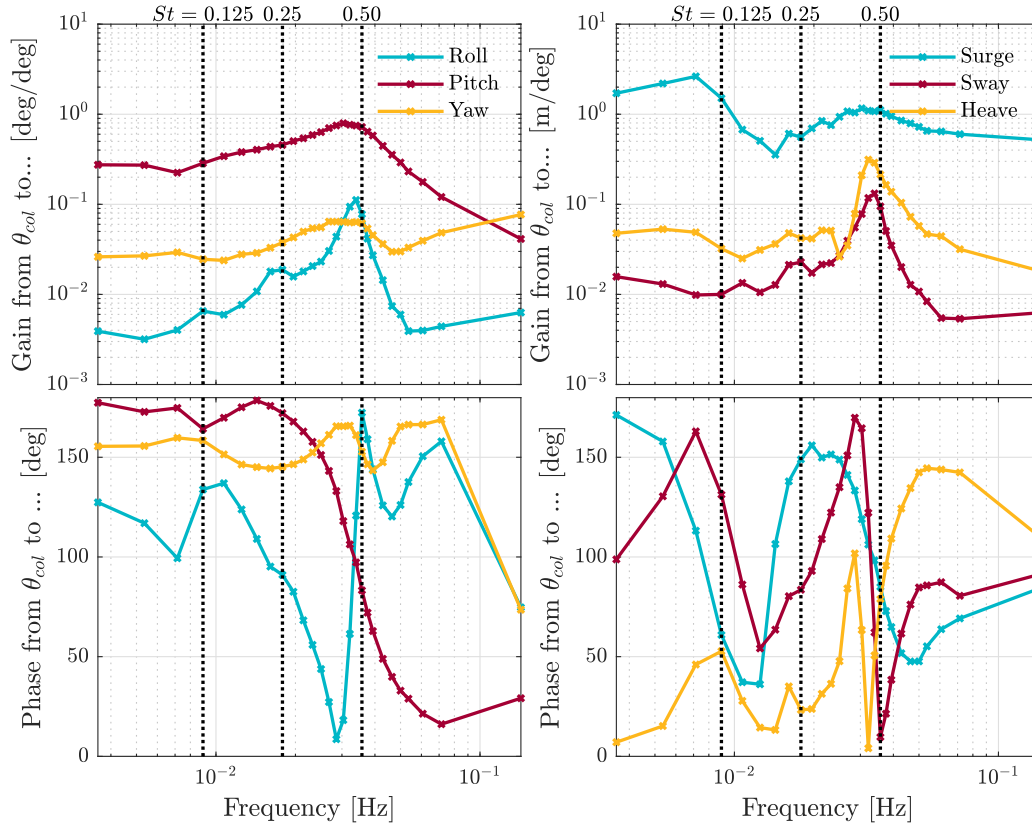
Figure 2. Frequency response functions for NREL 5 MW turbine on the OC3 spar-buoy platform. These frequency responses show all translational and rotational motions the turbine will undergo.

3.2.1 Platform Motions

Figure 2 shows the frequency responses for each of the degrees of freedom of a floating turbine. The turbine response shows that the type of motion that the floating turbine undergoes is dependent on the excitation frequency, with different movements becoming dominant at different frequencies. For example, while the surge motion is dominant at lower frequencies, the floating turbine undergoes a combination of pitching and surging motions at higher frequencies. All other motions typically appear with at least an order of magnitude lower amplitude than the surge or platform pitching motion. Therefore, they will be neglected in further analysis.

3.2.2 Effect on Nacelle Displacement

The motion of the nacelle is mainly dependent on the floater design (Lemmer et al., 2020). While generally it is expected that a surge and pitch motion results in a nacelle displacement, it is possible that the surge and pitch motion counteract each other,
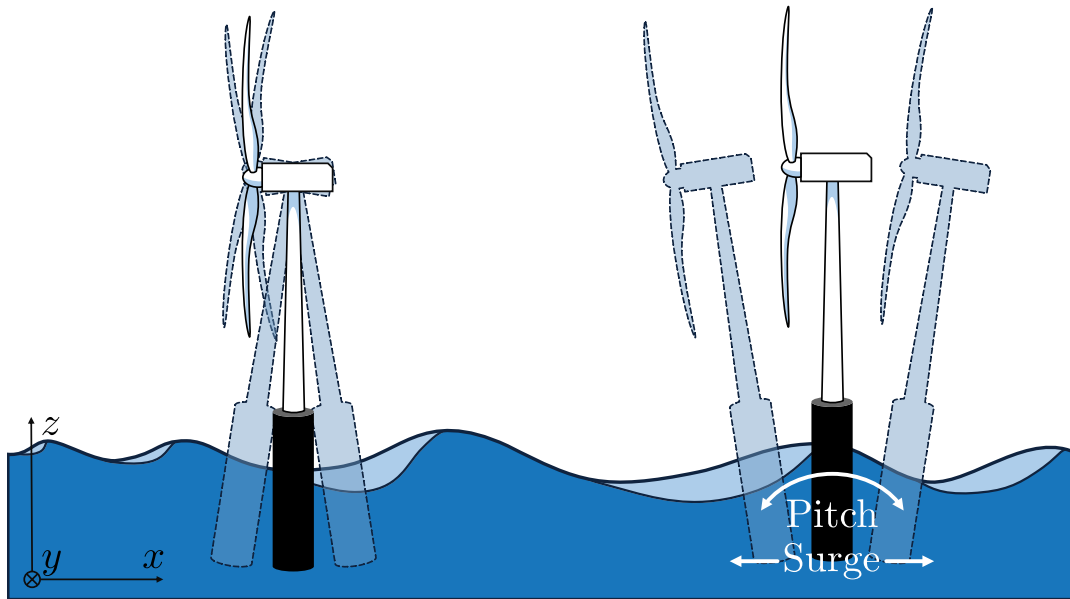
Figure 3. Two examples of floating turbines undergoing both surge and pitch motion resulting in different displacements of the nacelle.

causing the nacelle to remain almost stationary. An example of this is given in Figure 3: it depicts two floating turbines which are both pitching and surging whilst having different nacelle displacements. As will be shown in the frequency analysis, this is dependent on the phase and gain difference between the two motions. The movement of the nacelle is of interest as it will cause the turbine to experience a time-varying inflow and thus a time-varying thrust loading. It is expected that this may interfere
185   with the working principle of the Pulse. Therefore, the movement of the nacelle is also included in the frequency analysis. The frequency response diagrams for platform pitch, surge and nacelle motion are shown in Figure 4.

At low frequencies, that is until 0.01 [Hz], the motion of the nacelle is nearly one-to-one coupled to the surge motion, as the platform pitch angles are negligible. This can also be seen in the phase data, where the phase of the surge motion and nacelle motion are locked. Between 0.01 and 0.02 [Hz], the nacelle motion is the smallest for the frequency range considered.
190   Within this frequency range the platform surge and pitch motion are almost 180 degrees out of phase. This, combined with the lower surge motion, results in the floating turbine undergoing pitching and surging motion, without any significant nacelle displacement. This behaviour is depicted in the left situation of Figure 3. At its lowest point, the absolute gain from blade pitch angle to nacelle displacement is only 0.4 [m/deg], meaning for every degree of blade pitch angle the nacelle only moves by 40 centimetres. As frequency increases, the phase difference between surge and platform pitch diminishes and both motions
195   enhance the nacelle motion, graphically depicted in the right situation in Figure 3. This is most prominent at $St = 0.5$, where the nacelle motion achieves its second-to-maximum gain (the first being at a lower frequency).
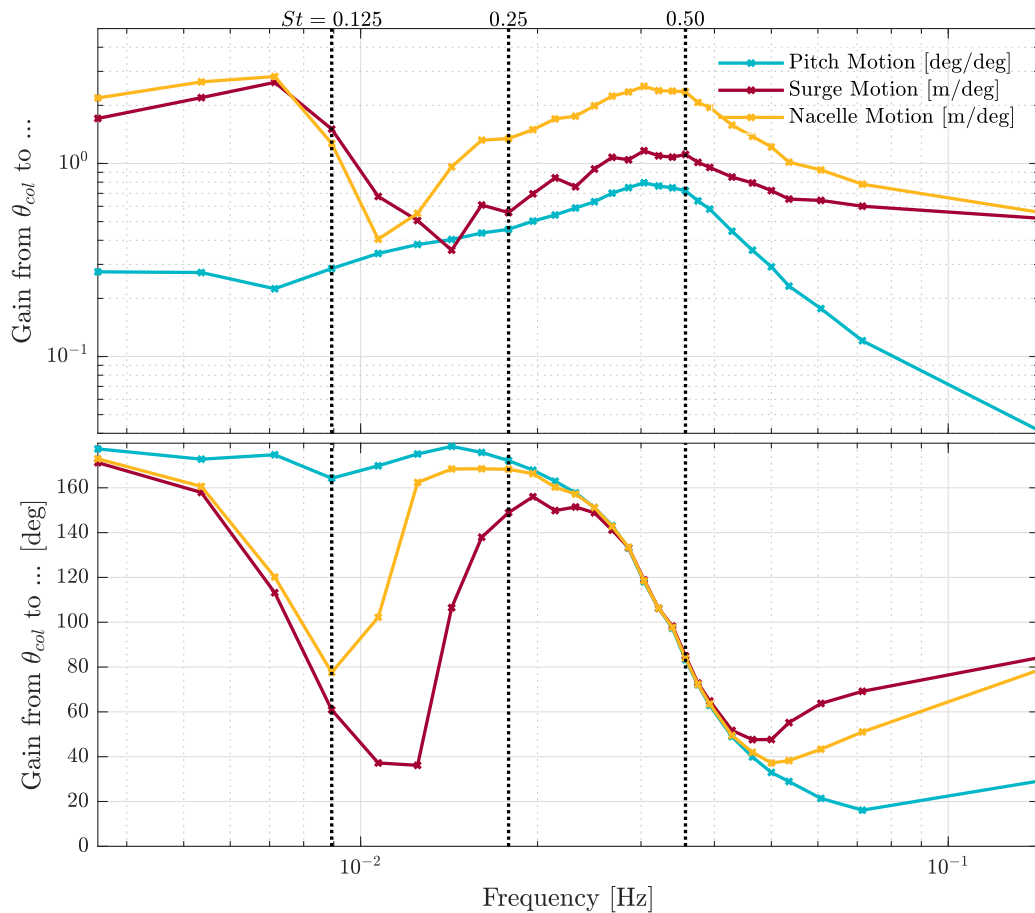
Figure 4. Frequency response functions for platform pitch, surge and nacelle motion for NREL 5 MW turbine on the OC3 spar-buoy platform.

3.2.3 Effect on Turbine Thrust

Up till this point, only the displacement of the floating turbine at different frequencies has been considered. For a bottom-fixed turbine the frequency, and blade pitching amplitude, at which the Pulse is applied, significantly impact the wake mixing behind the turbine. Typically, the frequency of $St = 0.25$ is taken as ideal when considering two aligned turbines spaced 5 rotor diameters apart (Munters and Meyers, 2018). It could be, however, that this is no longer the case for floating turbines, as the effect of the motion of the floating turbine has to be taken into account. It could well be that actuating at different frequencies on a floating turbine, yields different (local) optima.

One turbine parameter that provides insight into the expected wake mixing is the thrust force. By varying the thrust force, the wake is disturbed through the resulting time-varying wind field. As the turbine moves, it will experience a different relative
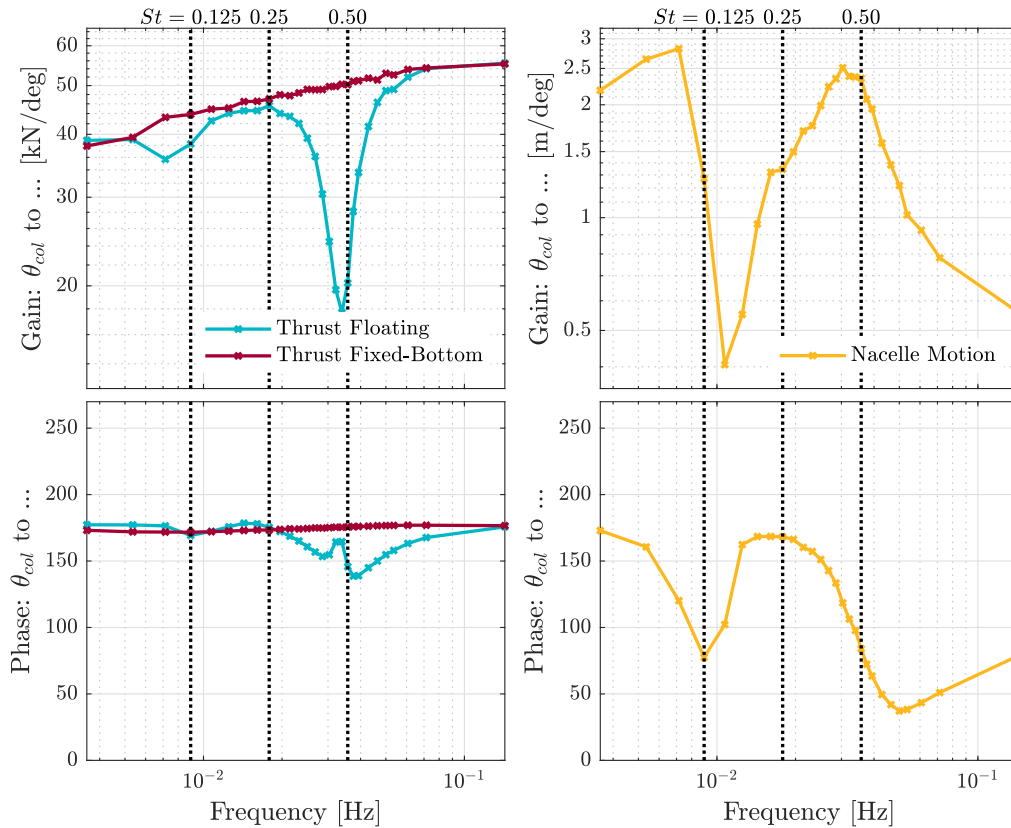
Figure 5. Frequency response functions for thrust force and nacelle motion, for NREL 5MW turbine on the OC3 spar-buoy platform.

wind speed, influencing the thrust force of the turbine. It could be that the extra dynamics could lead to locally higher, or lower, peaks in the thrust force variation. Figure 5 shows the frequency response of the thrust force as well as the nacelle motion.

Within Figure 5 two antiresonances can be identified in the floating thrust force. One is located at 0.008 [Hz] and a more prominent antiresonance is between 0.03 and 0.04 [Hz]. At both frequencies there is also a peak in the motion of the nacelle, indicating that there is indeed a coupling between platform and Pulse dynamics. This coupling, however, seems to have a negative impact, as in, as the motion of the nacelle increases the variation in thrust force decreases. The difference in the size of the antiresonance can be explained by considering the frequency at which the motion is at its maximum. The second peak occurs at ≈ 5 times the frequency of the first peak, which means the nacelle is moving with a higher velocity.

At $St = 0.25$ the opposite behaviour to the antiresonance frequencies can be seen. Here, the nacelle motion has an antiresonance and the thrust has a peak. At higher frequencies (> 0.06 [Hz]) the gain in thrust reaches its highest gain. However, it is also at this frequency that the Pulse becomes less effective as the blades are pitching at a too high frequency. The frequency area of interest is therefore between $St = 0.125$ and $St = 0.5$. Also included in Figure 5 is the gain from blade pitch angle to turbine thrust for a bottom fixed NREL 5MW turbine. At all frequencies, the gain for the bottom-fixed turbine is equal to or

greater than that of the floating turbine. At frequencies where the nacelle is not moving, or moving at low velocity, the gain

220 for thrust approaches that of the bottom-fixed turbine. At the resonance peaks of nacelle motion, there is a large difference in thrust force when compared to a bottom-fixed turbine.

The frequency analysis, as presented in this section, is a form of linear system analysis to describe how a system responds to an input signal with one distinct frequency. It fails to capture any non-linear dynamics in the system when the input signal is not a single sinusoid or the amplitude is time-varying. The full, potentially non-linear, behaviour of a floating wind turbine is

225 captured within the time domain simulations. Based on the frequency analysis it is clear that the nacelle motion has an effect on the time-varying thrust force. The full impact on the onset of wake mixing of the wake due to the nacelle motion and the physical displacement of the rotor plane is analyzed in the following section. Based on the thrust analysis it is expected that the movement will affect the onset of wake mixing.

4 Time Domain Results

230 This section investigates if the floating turbine movement for different Pulse frequencies has any noticeable impact on wake mixing. This is done by performing time domain simulations at three different Strouhal numbers: $St = 0.125$, $St = 0.25$ and $St = 0.5$ for both a bottom-fixed and floating turbine. The first and last frequencies correspond to a frequency where the floating turbine shows significant displacement. All floating turbine simulations are compared to a bottom-fixed turbine with the Pulse at the same frequency. First, the time domain results for nacelle displacement and corresponding thrust force will be shown

235 and discussed. Then, for each simulation, the average wind in the wake will be evaluated.

In total 8 different simulations are performed from which it is possible to evaluate downstream wind speeds at different locations. For these simulations, the settings as described in Section 2 are used. In each of the simulations, the turbine is floating unless stated otherwise. The eight simulations are:

1. Constant blade pitch angle (bottom-fixed baseline).

240 2. Constant blade pitch angle (floating baseline).

3. Pulse with $4°$ pitching amplitude at $St = 0.125$, bottom-fixed.

4. Pulse with $4°$ pitching amplitude at $St = 0.125$, floating.

5. Pulse with $4°$ pitching amplitude at $St = 0.250$, bottom-fixed.

6. Pulse with $4°$ pitching amplitude at $St = 0.250$, floating.

245 7. Pulse with $4°$ pitching amplitude at $St = 0.500$, bottom-fixed.

8. Pulse with $4°$ pitching amplitude at $St = 0.500$, floating.
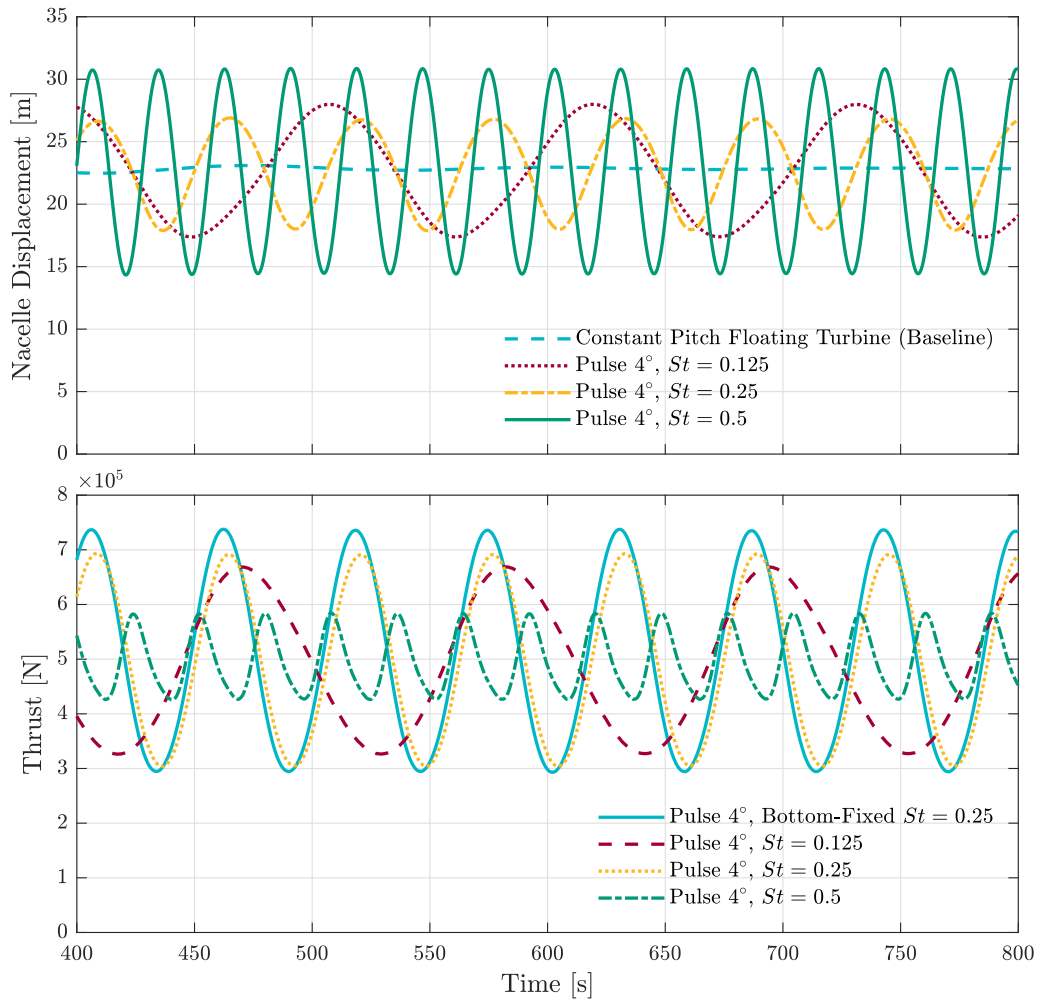
Figure 6. Time domain results for platform motion at three different Strouhal numbers. Each frequency has noticeable nacelle displacement which leads to differing behaviour in the thrust force.

4.1 Turbine Performance in Time Domain Simulations

Figure 6 shows the nacelle displacement as well as the resulting thrust for the three different frequencies considered. Alongside the data for the nacelle displacement, a simulation with a constant blade pitch angle is depicted for reference. This shows the

250 steady-state position around which the floating turbine is oscillating. For the thrust force data, a reference case with a bottom-fixed turbine excited with the Pulse at $St = 0.25$ is also included. At $St = 0.5$ the nacelle undergoes the largest displacement, with a total movement of 15 metres. As this occurs at the highest actuation frequency, it results in the highest velocity perceived by the nacelle. This combination of large amplitude and high frequency is of greater interest, as it equates to a larger fluctuation in relative wind speed.

255   The effect of this becomes apparent when looking at the thrust force of the turbine. For $St = 0.5$ the variation in thrust is significantly diminished compared to the bottom-fixed case. This observation is reinforced by looking at the $St = 0.125$ case. For that case, the total nacelle displacement is not significantly less than for $St = 0.5$, but due to the lower frequency, the variation in velocity experienced by the turbine will be substantially slower. This is reflected in the variance of the thrust force, which is larger compared to the $St = 0.5$ case. As this time-varying thrust force is the driving mechanism behind the Pulse, it

260 is expected that the lower peak-to-peak amplitude results in less wake mixing and thus lower downstream wind speeds.

    In conclusion, the lower peak-to-peak amplitude in the thrust force due to the platform motion can be compared to applying the Pulse to a bottom-fixed turbine, but with a smaller amplitude. This is likely reducing the overall effectiveness of the wake-mixing strategy.

4.2   Average Wind Speed Downstream

265 Thus far, the focus has primarily been on turbine performance and its, potential, relation to wake mixing dynamics. The time domain data confirms that the fluctuation of the thrust force varies significantly for different operating frequencies. Up to this point, it is hypothesized that this will affect the degree of wake mixing behind the turbine. This section analyzes the wind speed in the wake, another measure for wake mixing.
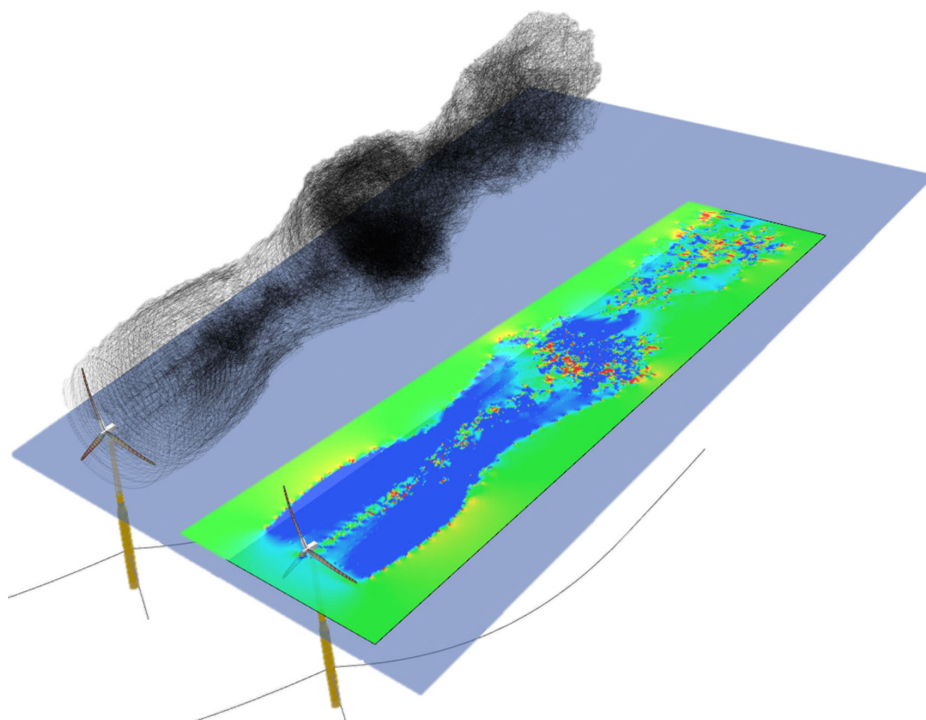
Figure 7. A screenshot from QBlade during one of the floating simulations. The velocity profile is only for illustrative purposes and not used for data analysis in this work.

For each simulation the wind speed is calculated at $0.5D$ distance spacing, starting $0.5D$ in front of the turbine up to $7D$ behind the turbine for a total of 16 velocity measurements. At each $0.5D$ a YZ-plane measuring 360 by 360 metres and centred at turbine level is exported for every 0.5 seconds. This plane is sectioned in squares of 3 by 3 metres yielding a grid of 120 by 120 individual velocity measurements. These dimensions were chosen such that wake expansion is fully captured over the entire domain. For each velocity plane, the average velocity experienced by a second NREL 5 MW turbine downstream, is computed for each time step for 10 minutes of data (1200 data points per simulation). An example of the wake and its velocity profile at hub height can be seen in Figure 7.

Figure 8 shows a comparison between cases with the same Pulse frequency and their respective baselines. Between the floating and bottom-fixed baseline there is, when averaged, no difference in downstream wind speed even though there is a slight difference in operating conditions. For the $St = 0.125$ and $St = 0.25$ cases, there is little difference between bottom-fixed and floating cases. At distances of $4D$ and higher, the floating $St = 0.125$ case does show lower wind speeds compared to their bottom-fixed counterpart. The most notable difference can be seen at $St = 0.5$. Over the entire distance of the considered domain, the wind speed remains lower compared to the bottom-fixed case. As seen in the previous section, it is also the frequency at which the largest peak-to-peak amplitude in thrust force is seen in the time data.

Figure 9 shows the same data but then all of the bottom-fixed and floating cases are compared with each other. Even though close to the turbine, there is a difference in average wind speed for the bottom-fixed cases, at a $5D$ distance, the wind speed has converged to nearly identical values. These findings are in line with the work presented in Munters and Meyers (2018). The same cannot be said for the floating cases, where the $St = 0.25$ outperforms both other pulse cases.

Based on the analysis presented in this section it is clear that the additional dynamics of a floating turbine do not necessarily lead to an increase in wake mixing. More importantly, one can conclude that when applying the Pulse whilst disregarding floater dynamics, it could lead to lower performance of the Pulse when applied to an otherwise identical bottom-fixed turbine. Recent work presented in Broek et al. (2022) confirms the findings in this section. In that work, an adjoint optimization is run to find the ideal Pulse signal for a 2-turbine floating wind farm. The optimal signal has a frequency which matches the frequency at which the nacelle is moving the least.

5   Conclusion

For bottom-fixed turbines, the effectiveness of the Pulse wake mixing strategy is dependent on both the application frequency as well as the amplitude of the sinusoidal signal. This work shows that the same holds for floating wind turbines. However, the turbine motion induced by the Pulse at different frequencies, predominately in the surge and pitching direction, will further influence its effectiveness and makes it more sensitive to frequency. The dynamic coupling between thrust and the resulting nacelle displacement is such that at certain frequencies the large nacelle displacement results in lower downstream wind speeds.

This nacelle displacement causes the turbine to experience a varying relative wind speed which negatively impacts the thrust force of the turbine. When the floating turbine is moving due to the Pulse, the movement is such that it lowers the peak-to-peak amplitude of the thrust force. Time domain simulations for three different frequencies show that this lowering of the peak-to-

WIND ENERGY SCIENCE DISCUSSIONS
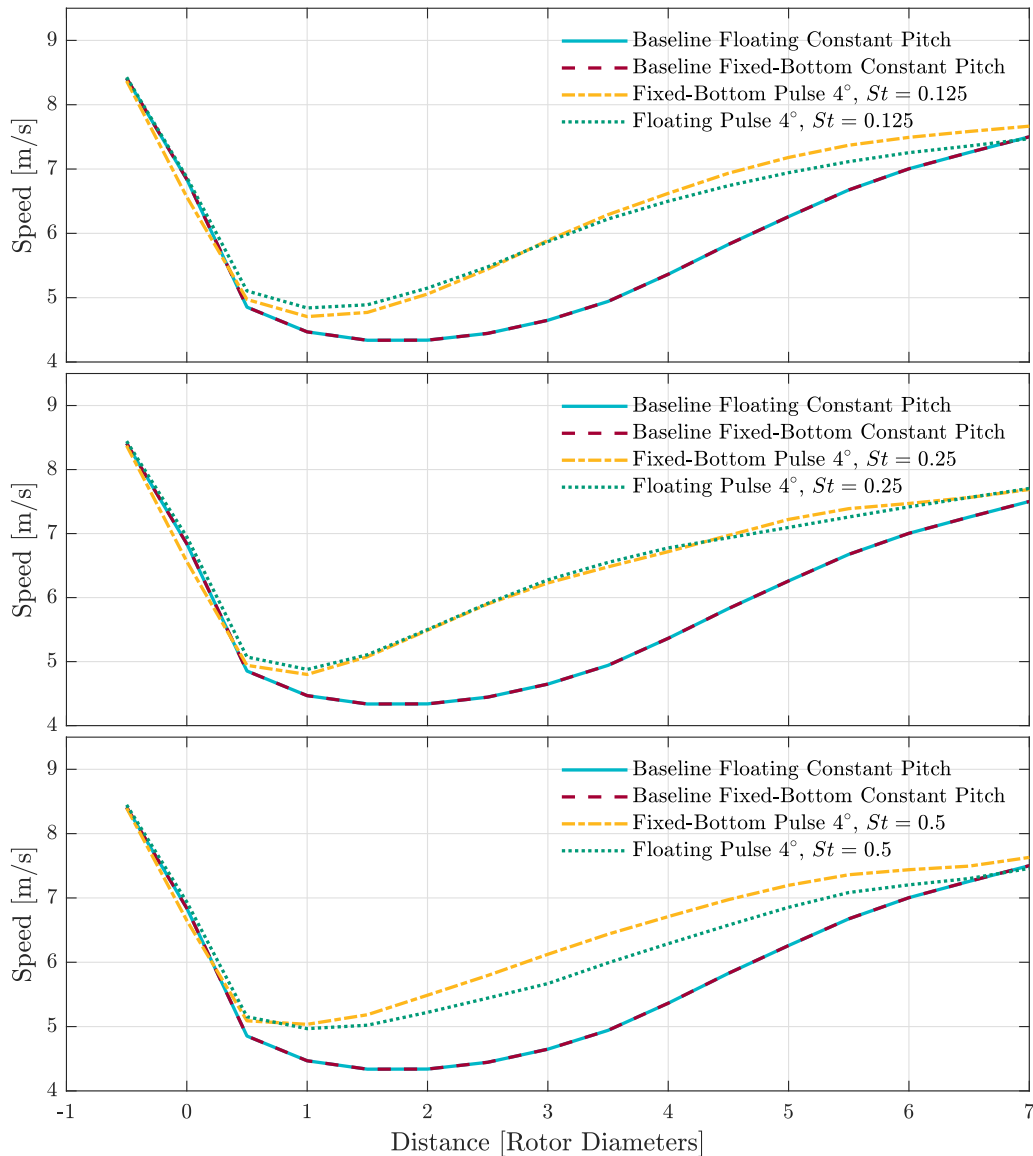
Figure 8. Average wind speeds over the analyzed domain for all simulations. Each floating simulation is compared to its bottom-fixed counterpart. Also included in the graphs are both baselines.

peak amplitude of the thrust force correlates to lower wind speeds downstream in the wake. This implies that the degree to which wake mixing occurs is lowered due to the movement of the floating turbine at certain frequencies.

The work presented in this paper shows that the coupling between wake mixing dynamics and floating turbine dynamics will present a new challenge in finding the right operating frequency, should the Pulse be deployed in a floating wind farm. With this specific floater turbine combination, movement is undesired from a wake mixing perspective. However, new floater
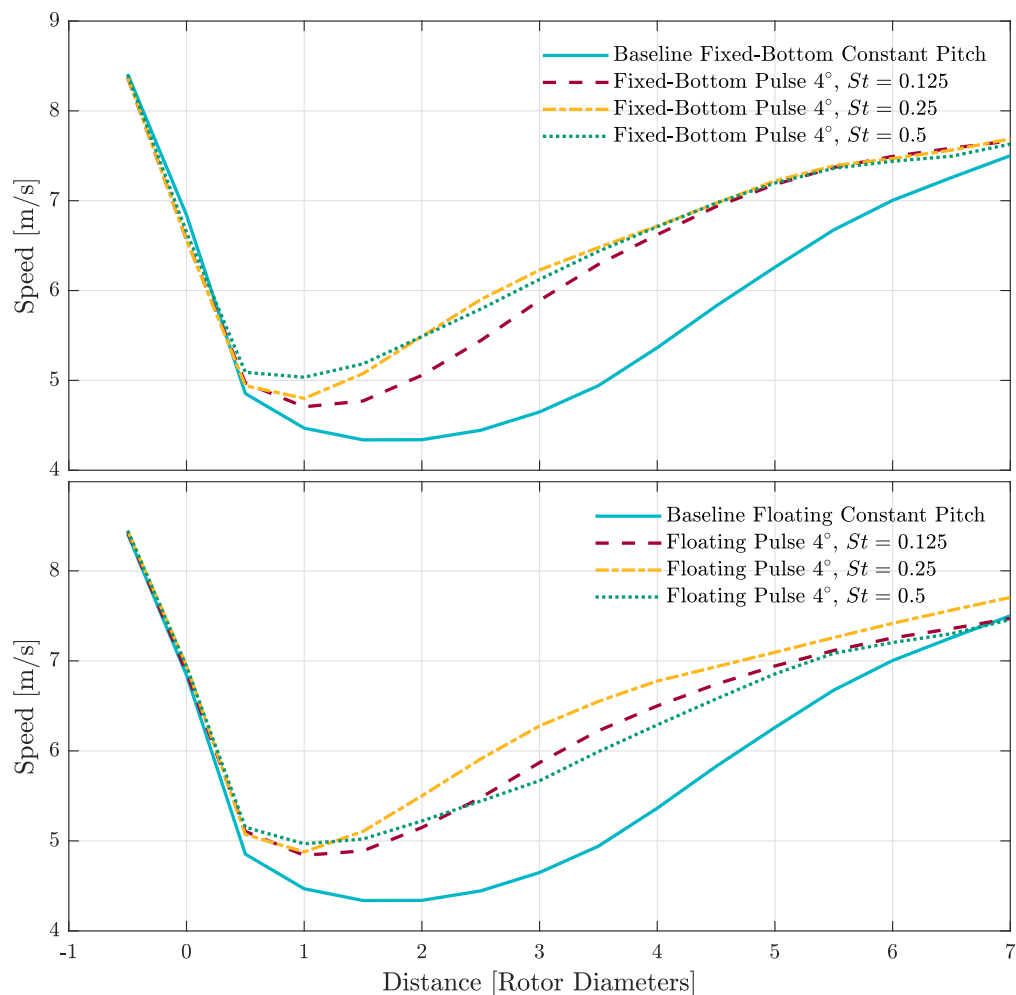
Figure 9. Average wind speed comparison between cases with the same mounting method. Where all bottom-fixed cases converge to the same wind speed, a difference between floating cases can be identified.

designs will also introduce different floating dynamics which might produce different results, or floaters could potentially be designed such that they are guaranteed to enhance wake mixing through their design.

6 Acknowledgements

310 This project is part of the Floatech project. The research presented in this paper has received funding from the European Union's Horizon 2020 research and innovation programme under grant agreement No. 101007142.
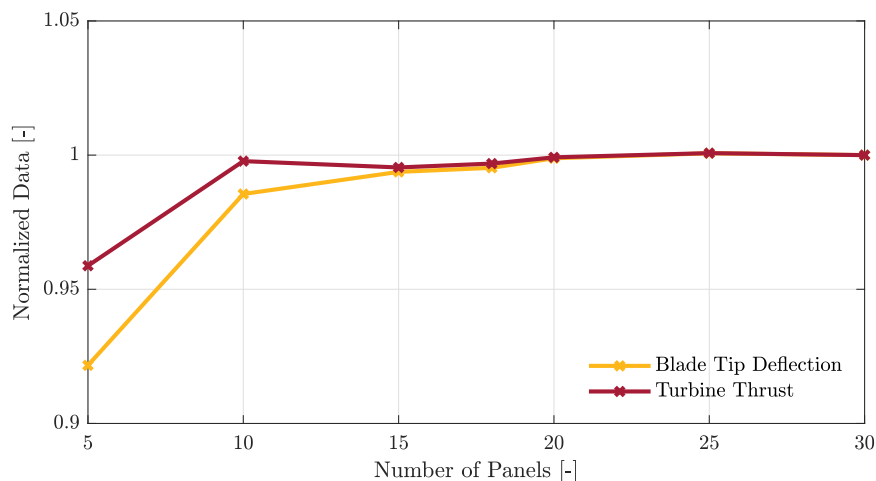
Figure A1. Selected results for the convergence results. The plot shows convergence for both an integral parameter (thrust) and an instantaneous parameter (blade tip deflection).

Appendix A: Convergence Study

This appendix covers the in-depth convergence study that was done to set the simulation settings used in this research. This convergence study focused on the effect that blade discretization has on turbine performance. Two parameters are analyzed, the turbine thrust and blade tip deflection. The first variable is key to being accurately resolved for the purpose of this research. The second variable is a direct result of the accuracy at which the aerodynamic force is resolved on the blade. Blade discretization also influences the number of vortex elements released into the wake (see Figure 1), which directly impacts computational time.

The results of the convergence study are shown in Figure A1. A blade discretization with 30 panels is chosen as the baseline, as it is likely this gives the most accurate representation of the turbine. As will be shown in the results, going higher than 30 yields diminishing marginal gains in terms of accuracy at the cost of computational time. All other data are presented as percentual differences with respect to it. The turbine thrust converges already at 10 panels. The blade tip deflection, however, converges at 15 panels or higher.

Furthermore, as the number of panels increases, so does the computational time. Ultimately the choice of the number of blade panels is a trade-off between the desired accuracy and computational time. *QBlade-Ocean* is provided with a model of the NREL5MW turbine in which the blade is discretized into 18 panels. A data point for 18 panels is also included in the convergence plot.

The effect of having different wake zones on the wake is also investigated. This is done by looking at the wind speed in the wake. Whenever the wake transitions from one zone to another, the number of vortex elements is reduced by interpolating among vortex elements and replacing them with a representative, new, vortex elements. Within *QBlade-Ocean* the length of a

315

320

325

330
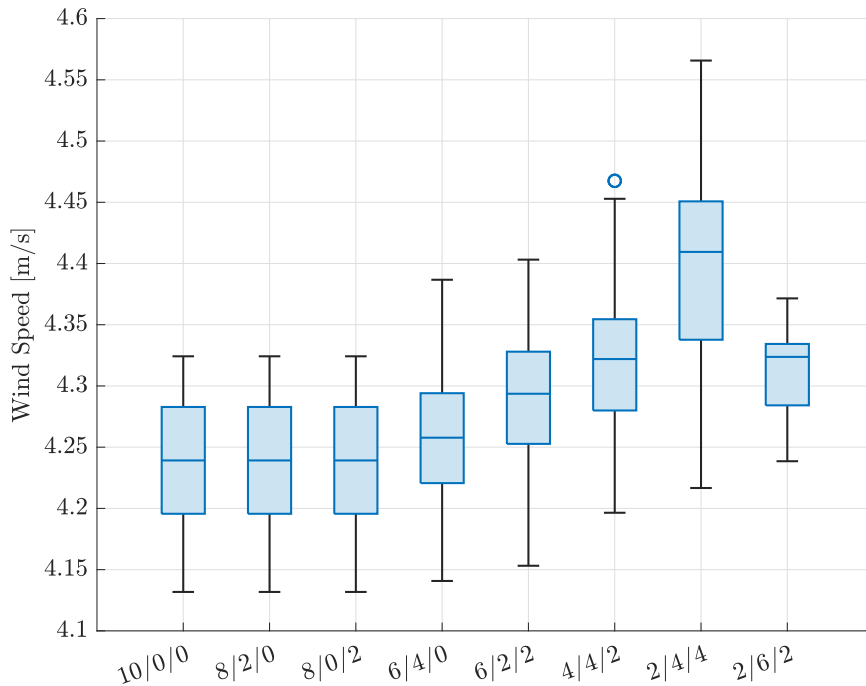
Figure B1. Average wind speeds downstream for different wake zones. The numbers on x-axis indicates the unit length of measure for Wake Zone 1/2/3 respectively. The 25th, 50th and 75th percentile are shown as a box. The bars indicate the distance to the, non-outlier, minima and maxima in the data set. Any circles indicate data outliers excluded in the boxplot.

wake zone is defined in the number of turbine revolutions. The total number of revolutions for all wake zones summed is kept at 10 for this investigation. A further half revolution is reserved for the near wake, which is a fully panelized wake and is visible in Figure 1. The influence of the different distributions of wake zones is analysed by looking at the velocity in the wake at a distance of 400 metres downstream. The results are presented in Figure B1. From the results in Figure B1, it is clear that there
335   is no difference between cases 1 to 3. This is likely due to the fact that the wake only transitions after the chosen distance of 8 wake zones. This is confirmed by looking at case 4, where the length of zone 2 is expanded. In that case, the velocity field fully falls in zone 2. This results in a slight increase in wind speed and a larger variance which implies that the wake is less stable. Transitioning to wake zone 3 further increases the downstream wind speed and corresponding variance. The biggest takeaway is that allowing the wake to transition to zone 2 impacts the stability of the wake slightly and results in a small increase in
340   wind speed. However, keeping the velocity field of interest in zone 2 seems to provide a good trade-off between accuracy and computational time. Therefore, the wake zones chosen for this research, as presented in Table 2, are chosen such that the wind field fully falls into zone 2 whilst also allowing zone 1 enough time to fully develop.

Author contributions. DVDB set-up and processed all simulations that led to the results presented in this paper under the supervision of DDT and JWVW. The insights and conclusions presented in this paper are the results of extensive discussions among the three authors.

345 *Competing interests.* The authors have the following competing interests: At least one of the (co-)authors is a member of the editorial board of Wind Energy Science.

References

Ananthan, S. and Leishman, J. G.: Role of Filament Strain in the Free-Vortex Modeling of Rotor Wakes, Journal of the American Helicopter Society, 49, 176–191, https://doi.org/10.4050/JAHS.49.176, 2004.

350 Astrom, K. J. and Murray, R. M.: Feedback Systems: An Introduction for Scientists and Engineers, Princeton University Press, USA, 2008.

Barthelmie, R. J., Hansen, K., Frandsen, S. T., Rathmann, O., Schepers, J. G., Schlez, W., Phillips, J., Rados, K., Zervos, A., Politis, E. S., and Chaviaropoulos, P. K.: Modelling and measuring flow and wind turbine wakes in large wind farms offshore, Wind Energy, 12, 431–444, https://doi.org/10.1002/we.348, 2009.

Barthelmie, R. J., Pryor, S. C., Frandsen, S. T., Hansen, K. S., Schepers, J. G., Rados, K., Schlez, W., Neubert, A., Jensen, L. E., and
355 Neckelmann, S.: Quantifying the Impact of Wind Turbine Wakes on Power Output at Offshore Wind Farms, Journal of Atmospheric and Oceanic Technology, 27, 1302–1317, https://doi.org/10.1175/2010JTECHA1398.1, publisher: American Meteorological Society Section: Journal of Atmospheric and Oceanic Technology, 2010.

Bastankhah, M. and Porté-Agel, F.: Experimental and theoretical study of wind turbine wakes in yawed conditions, Journal of Fluid Mechanics, 806, 506–541, https://doi.org/10.1017/jfm.2016.595, 2016.

360 Becker, M., Ritter, B., Doekemeijer, B., van der Hoek, D., Konigorski, U., Allaerts, D., and van Wingerden, J. W.: The revised FLORIDyn model: implementation of heterogeneous flow and the Gaussian wake, Wind Energy Science, 7, 2163–2179, https://doi.org/10.5194/wes-7-2163-2022, 2022.

Berdowski, T.: Three-Dimensional Free-Wake Vortex Simulations of an Actuator Disc in Yaw and Tilt, https://doi.org/10.2514/6.2018-0513, 2018.

365 Broek, M. J. v. d., Berg, D. v. d., Sanderse, B., and van Wingerden, J. W.: Optimal Control for Wind Turbine Wake Mixing on Floating Platforms, https://doi.org/10.48550/ARXIV.2210.17347, 2022.

Campagnolo, F., Petrovic, V., Bottasso, C., and Croce, A.: Wind tunnel testing of wake control strategies, in: 2016 American Control Conference (ACC), pp. 513–518, https://doi.org/10.1109/ACC.2016.7524965, 2016.

Ciri, U., Rotea, M. A., and Leonardi, S.: Model-free control of wind farms: A comparative study between individual and coordinated
370 extremum seeking, Renewable Energy, 113, 1033–1045, https://doi.org/10.1016/j.renene.2017.06.065, 2017.

European Commission: Information on the REPowerEU initiative., https://ec.europa.eu/info/strategy/priorities-2019-2024/european-green-deal/repowereu-affordable-secure-and-sustainable-energy-europe_en, 2022.

Fleming, P., Gebraad, P. M. O., Lee, S., van Wingerden, J. W., Johnson, K., Churchfield, M., Michalakes, J., Spalart, P., and Moriarty, P.: Simulation comparison of wake mitigation control strategies for a two-turbine case, Wind Energy, 18, 2135–2143,
375 https://doi.org/https://doi.org/10.1002/we.1810, 2015.

Fleming, P., Annoni, J., Shah, J. J., Wang, L., Ananthan, S., Zhang, Z., Hutchings, K., Wang, P., Chen, W., and Chen, L.: Field test of wake steering at an offshore wind farm, Wind Energy Science, 2, 229–239, https://doi.org/10.5194/wes-2-229-2017, 2017.

Floatech: Floatech Project Website, https://www.floatech-project.com, 2022.

Frederik, J. A., Doekemeijer, B. M., Mulders, S. P., and van Wingerden, J. W.: The helix approach: Using dynamic individual pitch control
380 to enhance wake mixing in wind farms, Wind Energy, 23, 1739–1751, https://doi.org/https://doi.org/10.1002/we.2513, 2020a.

Frederik, J. A., Weber, R., Cacciola, S., Campagnolo, F., Croce, A., Bottasso, C., and van Wingerden, J. W.: Periodic dynamic induction control of wind farms: proving the potential in simulations and wind tunnel experiments, Wind Energy Science, 5, 245–257, https://doi.org/10.5194/wes-5-245-2020, 2020b.

Gebraad, P. and van Wingerden, J. W.: A Control-Oriented Dynamic Model for Wakes in Wind Plants, in: Journal of Physics: Conference

385   Series, pp. 1848–1857, https://doi.org/10.1088/1742-6596/524/1/012186, 2014.

Gebraad, P. M. O., Teeuwisse, F. W., van Wingerden, J. W., Fleming, P. A., Ruben, S. D., Marden, J. R., and Pao, L. Y.: Wind plant
     power optimization through yaw control using a parametric model for wake effects—a CFD simulation study, Wind Energy, 19, 95–114,
     https://doi.org/https://doi.org/10.1002/we.1822, 2016.

Goit, J. and Meyers, J.: Optimal control of energy extraction in wind-farm boundary layers, Journal of Fluid Mechanics, 768, 5–50,

390   https://doi.org/10.1017/jfm.2015.70, 2015.

Han, C. and Nagamune, R.: Platform position control of floating wind turbines using aerodynamic force, Renewable Energy, 151, 896–907,
     https://doi.org/10.1016/j.renene.2019.11.079, 2020.

Jensen, N. O.: A note on wind generator interaction, no. 2411 in Risø-M, Risø National Laboratory, 1983.

Jiménez, A., Crespo, A., and Migoya, E.: Application of a LES technique to characterize the wake deflection of a wind turbine in yaw, Wind

395   Energy, 13, 559–572, https://doi.org/https://doi.org/10.1002/we.380, 2010.

Jonkman, J.: Definition of the Floating System for Phase IV of OC3, https://doi.org/10.2172/979456, 2010.

Jonkman, J., Butterfield, S., Musial, W., and Scott, G.: Definition of a 5-MW Reference Wind Turbine for Offshore System Development,
     https://doi.org/10.2172/947422, 2009.

Kheirabadi, A. C. and Nagamune, R.: Real-time relocation of floating offshore wind turbine platforms for wind farm efficiency maximization:

400   An assessment of feasibility and steady-state potential, Ocean Engineering, 208, 107 445, https://doi.org/10.1016/j.oceaneng.2020.107445,
     2020.

Kirchner-Bossi, N. and Porté-Agel, F.: Realistic Wind Farm Layout Optimization through Genetic Algorithms Using a Gaussian Wake
     Model, Energies, 11, 3268, https://doi.org/10.3390/en11123268, 2018.

Komusanac, I., Brindley, G., Fraile, D., and Ramirez, L.: WindEurope Annual Statistics 2021, https://windeurope.org/intelligence-platform/

405   product/wind-energy-in-europe-2021-statistics-and-the-outlook-for-2022-2026/, 2021.

Leishman, J., Beddoes, T. S., and Ltd, W. H.: A Generalised Model for Airfoil Unsteady Aerodynamic Behaviour and Dynamic Stall Using
     the Indicial Method, Presented at the 42nd. Annual Forum of the American Helicopter Society, 1986.

Leishman, J. G., Bhagwat, M. J., and Bagai, A.: Free-Vortex Filament Methods for the Analysis of Helicopter Rotor Wakes, Journal of
     Aircraft, 39, 759–775, https://doi.org/10.2514/2.3022, 2002.

410 Leishman, J. G., Bhagwat, M. J., and Ananthan, S.: The Vortex Ring State as a Spatially and Temporally Developing Wake Instability,
     Journal of the American Helicopter Society, 49, 160–175, https://doi.org/10.4050/JAHS.49.160, 2004.

Lemmer, F., Yu, W., Müller, K., and Cheng, P. W.: Semi-submersible wind turbine hull shape design for a favorable system response behavior,
     Marine Structures, 71, 102 725, https://doi.org/https://doi.org/10.1016/j.marstruc.2020.102725, 2020.

Marden, J. R., Ruben, S. D., and Pao, L. Y.: A Model-Free Approach to Wind Farm Control Using Game Theoretic Methods, in: IEEE

415   Transactions on Control Systems Technology, pp. 1207–1214, https://doi.org/10.1109/TCST.2013.2257780, 2013.

Marten, D.: Qblade Website, http://www.q-blade.org, 2022.

Marten, D., Paschereit, C. O., Huang, X., Meinke, M., Schröder, W., Müller, J., and Oberleithner, K.: Predicting Wind Turbine Wake Break-
     down Using a Free Vortex Wake Code, AIAA Journal, 58, 4672–4685, https://doi.org/10.2514/1.J058308, 2020.

Meyers, J., Bottasso, C., Dykes, K., Fleming, P., Gebraad, P., Giebel, G., Göçmen, T., and van Wingerden, J. W.: Wind farm flow control:

420   prospects and challenges, Wind Energy Science Discussions, 2022, 1–56, https://doi.org/10.5194/wes-2022-24, 2022.

Mosetti, G., Poloni, C., and Diviacco, B.: Optimization of wind turbine positioning in large windfarms by means of a genetic algorithm, Wind Engineering and Industrial Aerodynamics, 51, 105–116, https://doi.org/10.1016/0167-6105(94)90080-9, 1994.

Munters, W. and Meyers, J.: Effect of wind turbine response time on optimal dynamic induction control of wind farms, in: Journal of Physics: Conference Series, p. 052007, https://doi.org/10.1088/1742-6596/753/5/052007, 2016.

425 Munters, W. and Meyers, J.: Towards practical dynamic induction control of wind farms: analysis of optimally controlled wind-farm boundary layers and sinusoidal induction control of first-row turbines, Wind Energy Science, 3, 409–425, https://doi.org/10.5194/wes-3-409-2018, 2018.

Nanos, E. M., Letizia, S., Clemente, D. J. B., Wang, C., Rotea, M., Iungo, V. I., and Bottasso, C. L.: Vertical wake deflection for offshore floating wind turbines by differential ballast control, in: Journal of Physics: Conference Series, p. 022047, https://doi.org/10.1088/1742-6596/1618/2/022047, 2020.

430 Panwara, N. L., Kaushikb, S. C., and Kotharia, S.: Role of renewable energy sources in environmental protection: A review, Renewable and Sustainable Energy Reviews, 15, 1513–1524, 2011.

Pereira, R., Schepers, G., and Pavel, M. D.: Validation of the Beddoes–Leishman dynamic stall model for horizontal axis wind turbines using MEXICO data, Wind Energy, 16, 207–219, https://doi.org/10.1002/we.541, 2013.

435 Petersen, E. L., Mortensen, N. G., Landberg, L., Højstrup, J., and Frank, H. P.: Wind power meteorology. Part I: climate and turbulence, Wind Energy, 1, 25–45, https://doi.org/10.1002/(SICI)1099-1824(199804)1:1+<25::AID-WE4>3.0.CO;2-D, 1998.

Ramirez, L., Fraille, D., and Brindley, G.: The European offshore wind industry - key trends and statistics 2020, https://windeurope.org/intelligence-platform/product/offshore-wind-in-europe-key-trends-and-statistics-2020/, 2020.

Rodrigues, S. F., Teixeira Pinto, R., Soleimanzadeh, M., Bosman, P. A. N., and Bauer, P.: Wake losses optimization
440 of offshore wind farms with moveable floating wind turbines, Energy Conversion and Management, 89, 933–941, https://doi.org/10.1016/j.enconman.2014.11.005, 2015.

Rodriguez, S. N., Jaworski, J. W., and Michopoulos, J. G.: Stability of helical vortex structures shed from flexible rotors, Journal of Fluids and Structures, 104, 103 279, https://doi.org/10.1016/j.jfluidstructs.2021.103279, 2021.

Shaler, K., Branlard, E., Platt, A., and Jonkman, J.: Preliminary Introduction of a Free Vortex Wake Method Into OpenFAST, Journal of
445 Physics: Conference Series, 1452, 012 064, https://doi.org/10.1088/1742-6596/1452/1/012064, 2020.

van den Berg, D., de Tavernier, D., and van Wingerden, J. W.: Using The Helix Mixing Approach on Floating Offshore Wind Turbines, Journal of Physics: Conference Series, 2265, 042 011, https://doi.org/https://doi.org/10.1088/1742-6596/2265/4/042011, 2022.

van der Hoek, D., Kanev, S., Allin, J., Bieniek, D., and Mittelmeier, N.: Effects of axial induction control on wind farm energy production - A field test, Renewable Energy, 140, 994–1003, https://doi.org/10.1016/j.renene.2019.03.117, 2019.

450 WindEurope: Floating Offshore Wind Vision Statement, https://windeurope.org/about-wind/reports/floating-vision-statement/, 2017.